In Vitro Actin Filament Sliding Velocities Produced by Mixtures of Different Types of Myosin

G. Cuda,*¶ E. Pate,# R. Cooke,§ and J. R. Sellers*

*Laboratory of Molecular Cardiology, National Heart, Lung, and Blood Institute, National Institutes of Health, Bethesda, Maryland 20892 USA; #Department of Pure and Applied Mathematics, Washington State University, Pullman, Washington 99164 USA; §Department of Biochemistry and Biophysics and CVRI, University of California, San Francisco, California 94143 USA; and ¶Dipartmento di Medicina Sperimentale e Clinica, Facolta di Medicina di Catanzaro, Policlinico Mater Domini, 88100 Catanzaro, Italy

ABSTRACT Using in vitro motility assays, we examined the sliding velocity of actin filaments generated by pairwise mixings of six different types of actively cycling myosins. In isolation, the six myosins translocated actin filaments at differing velocities. We found that only small proportions of a more slowly translating myosin type could significantly inhibit the sliding velocity generated by a myosin type that translocated filaments rapidly. In other experiments, the addition of noncycling, unphosphorylated smooth and nonmuscle myosin to actively translating myosin also inhibited the rapid sliding velocity, but to a significantly reduced extent. The data were analyzed in terms of a model derived from the original working cross-bridge model of A. F. Huxley. We found that the inhibition of rapidly translating myosins by slowly cycling was primarily dependent upon only a single parameter, the cross-bridge detachment rate at the end of the working powerstroke. In contrast, the inhibition induced by the presence of noncycling, unphosphorylated myosins required a change in another parameter, the transition rate from the weakly attached actomyosin state to the strongly attached state at the beginning of the cross-bridge power stroke.

INTRODUCTION

The sliding actin in vitro motility assay has proved useful for studying the interaction between actin and myosin (Kron and Spudich, 1986). It is thought to be an in vitro correlate of the unloaded shortening velocity of muscle fibers. In this assay, the movement of rhodamine-phalloidin-labeled actin filaments over a surface coated with myosin molecules is observed by video microscopy. The viscous drag on a sliding actin filament is significantly less than the mechanical force produced by the myosin cross-bridges. Thus the filaments are sliding at maximum velocities.

The observed velocity is dependent on the source of myosin, with a large range of velocities having been reported (Kron and Spudich, 1986; Umemoto and Sellers, 1990; Okagaki et al., 1989; Sellers and Kachar, 1990; Yamashita et al., 1992; Ganguly et al., 1992; Wang et al., 1993b; Sellers and Goodson, 1995). The source of actin, on the other hand, has little effect on sliding velocity (Umemoto and Sellers, 1990; Harris and Warshaw, 1993a). Warshaw et al. (1990) demonstrated that when slowly cycling phosphorylated smooth muscle myosin was mixed with the rapidly cycling skeletal muscle myosin, the velocity was markedly decreased by the slower smooth muscle myosin. Both smooth muscle myosin and nonmuscle myosin require phosphorylation of their regulatory light chains for activity (see Sellers and Goodson, 1995, for a review). Even though the unphosphorylated myosin does not have an actin-activated ATPase rate, and thus in isolation does not translocate actin filaments, it does interact with actin, probably in a weakly bound state (Sellers, 1985). We will refer to unphosphorylated smooth muscle and nonmuscle myosins as "noncycling" myosins. It has been shown that unphosphorylated, noncycling, smooth muscle myosin also slows the movement generated by actively cycling myosins. These experiments were extended and the data modeled in a later paper (Harris et al., 1994). Similar behavior was previously observed in another in vitro motility assay, where the movements of myosin filaments bound to polymer beads were measured over an oriented array of actin filaments derived from the microdissection of *Nitella axillaris* (Sellers et al., 1985).

In the present work we have extended these observations to more combinations of myosin types. Thus we have been able to obtain a wider range of actin filament sliding velocities in paired mixing experiments with actively cycling myosins. In addition, we have studied the effect of a varying fraction of noncycling, unphosphorylated smooth and nonmuscle myosins on the movement of actin filaments generated by cycling myosins. The experimental data were analyzed by computer simulation of a multistate cross-bridge model based on the original cross-bridge model of Huxley (1957). In the model, initial cross-bridge attachment was in a weakly attached, low-force state. After transition to a strongly bound, high-force state, an attached cross-bridge executed a power stroke, causing a relative displacement of the actin filament. When continued attachment after the power stroke would present a resistive force (the drag stroke), the cross-bridge detachment rate was assumed to rapidly increase and cross-bridges detached to begin a new cycle. We found that if only the cross-bridge detachment

Received for publication 12 April 1996 and in final form 16 January 1997.

Address reprint requests to Dr. James R. Sellers, National Institutes of Health, Bldg. 10, Room 8N-202, Bethesda, MD 20892-1762. Tel.: 301-496-6887; Fax: 301-402-1542; E-mail: jsellers@helix.nih.gov.

0006-3495/97/04/1767/13 $2.00

rate constant in the drag stroke region was varied, the model provided excellent agreement with our experimental results when two cycling myosins were mixed. The ability of noncycling myosin to retard the velocity of cycling myosin could also be simulated by decreasing only the rate constant for the transition between the weakly and strongly bound states of myosin.

MATERIALS AND METHODS

Preparation of proteins

All procedures were performed at 4°C. Turkey gizzard smooth muscle myosin (Umemoto et al., 1989), rabbit skeletal muscle myosin (Margossian and Lowey, 1982), and human platelet myosin (Daniel and Sellers, 1992) were prepared as previously described. Rat fast skeletal muscle myosin and bovine atrial and ventricular cardiac myosins were prepared by ammonium sulfate fraction of a high salt extracted actomyosin solution similar to that described for smooth muscle myosin (Umemoto et al., 1989). All myosins were used within 1 week of purification. Turkey gizzard tropomyosin (Umemoto et al., 1989), myosin light-chain kinase (Adelstein and Klee, 1981), rabbit skeletal muscle actin (Eisenberg and Kielley, 1974), and bovine brain calmodulin (Klee, 1977) were prepared by previously described methods. Turkey gizzard smooth muscle myosin and human platelet nonmuscle myosin were phosphorylated (Umemoto and Sellers, 1990), and the extent of phosphorylation was determined by urea-glycerol gel electrophoresis (Perrie and Perry, 1970).

In vitro motility assay

The sliding actin in vitro motility assay was performed as described previously (Homsher et al., 1992). The assay conditions were 20 mM KCl, 10 mM 3-(*N*-morpholino)propanesulfonic acid (pH 7.2), 5 mM $MgCl_2$, 1 mM ATP, 0.1 mM EGTA, 2 mM dithiothreitol, 0.7% methylcellulose, 2.5 mg/ml glucose, 0.1 mg/ml glucose oxidase, 0.02 mg/ml catalase, and 40 nM turkey gizzard tropomyosin. The latter three reagents retarded photobleaching of rhodamine phalloidin-labeled actin filaments. The presence of methylcellulose in the assay was needed to observe the movement of actin filaments by smooth muscle myosin. It also improved the quality of movement in the other samples. The temperature of the mixing experiments in the in vitro motility assay was 30°C.

In mixing experiments, the total myosin concentration added to the flow cell was maintained at 0.2 mg/ml while the ratio of the two myosins was varied. In all cases, myosins were added in 0.5 M NaCl, 10 mM 3-(*N*-morpholino)propanesulfonic acid (pH 7.0), 0.1 mM EGTA, 1 mM dithiothreitol, 3 mM NaN_3 and subsequently washed out with the above buffer containing 0.5 mg/ml bovine serum albumin. Under these conditions, myosin bound to the nitrocellulose surface as monomers.

The imaging and recording system, and the method of quantitation of actin filament sliding velocity were described previously (Homsher et al., 1992). Velocities are given as mean ± SD.

Modeling

We employed a three-state model that incorporated the essentials of current hypotheses regarding the cross-bridge cycle while maintaining computational tractability (see the Discussion for more details). The initial attachment of myosin to actin was assumed to be in a weakly bound, pre-power-stroke state. During active sliding, there was a subsequent transition to a strongly bound, working, power-stroke state. After the end of the power stroke, when continued attachment of the linearly elastic cross-bridge would inhibit useful work, cross-bridges detached and the cycle began again.

The computer model followed the basic framework of Huxley (1957), as elaborated by Eisenberg et al. (1980). The distance between a myosin cross-bridge and the nearest actin site is denoted by the variable x. The probability of cross-bridge attachment and detachment, and transition rates between attached states were assumed to depend upon the spatial variable x. Attached cross-bridges were taken to be linearly elastic structures, with the force proportional to the difference between the strain, x, and a neutral strain position. To fix notation, let $i = 1$, 2, and 3, respectively, designate the detached, weakly attached, and strongly attached states. Let $G_i(x)$ be the free energy of state i at strain x. For linearly elastic cross-bridges, the free energy of an attached state is parabolic in x. We assume the following free energies (units of kT, k is the Boltzmann constant and T is the absolute temperature):

$$G_1(x) = 0 \qquad G_2(x) = -2 + 0.5\kappa(x-7)^2$$
$$G_3(x) = -20 + 0.5\kappa x^2, \tag{1}$$

where $\kappa = 0.82kT/\text{nm}^2$ is the cross-bridge elastic force constant. Except as subsequently discussed, all myosin types have the same elastic force constant. Note that the neutral strain positions of the weakly and strongly attached states are different, $x = 7$ and 0 nm, respectively. The free energy profiles are plotted in Fig. 1, assuming that $\Delta G_{ATP} = 23kT$. Transition rate functions are initially taken as

$$R_{12}\begin{cases} = 5 + 10^5\exp[-2(7-x)^2] & x \geq 0 \\ = 0.001 & x < 0 \end{cases}$$
$$R_{23}\begin{cases} = 125\alpha & x \geq 7 \\ = [125 + 875(7-x)]\alpha & x < 7 \end{cases} \tag{2}$$
$$R_{31}\begin{cases} = 0.001 & x \geq 0 \\ = 1900\beta & x < 0. \end{cases}$$

Here α and β are scaling constants that are taken to depend upon myosin type. They are the parameters to be modified for fitting experimental data. The reverse transition rates between any two states, i and j, satisfy $R_{ij}(x)/R_{ji}(x) = \exp[(G_i(x) - G_j(x))/kT]$ to maintain thermodynamic consistency. Although not physically realistic, we have followed the method of Huxley (1957) in allowing jump discontinuities in the rate functions. Smoothing protocols are discussed by Pate and Cooke (1989).

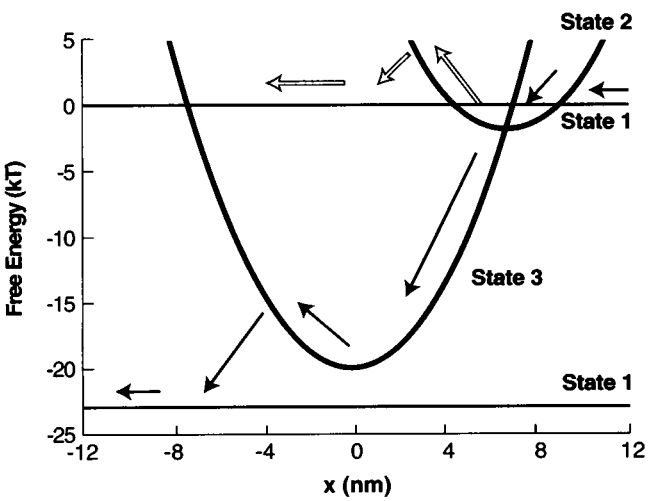

FIGURE 1 Free energy diagram for the working cross-bridge model used to analyze experimental data. Attached cross-bridges have parabolic free energy profiles (linearly elastic elements). Actin binding sites enter from the right. The solid arrows show the chemomechanical pathway of actively cycling cross-bridges. The open arrows show the alternative detachment pathway used by noncycling, weakly bound cross-bridges. Additional details are provided in Materials and Methods and the Discussion.

A more realistic five-state cross-bridge model has previously been considered, incorporating an additional detached state and an additional power-stroke state (Pate and Cooke, 1989). This model was optimized to explain experimental data on the effects of variation in substrate and hydrolysis products on contracting glycerinated rabbit psoas fibers (fast muscle) at 10°C. It provided the basic framework for the present analysis in that the shapes of the free energy profiles and transition rate functions between detached, weakly attached, and strongly attached states in the present analysis were similar to the rate-limiting steps for sliding velocity in the five-state analysis. The rate functions (Eq. 2) were optimized so that the values $\alpha = \beta = 1.0$ gave the best fit for the mean sliding velocity observed in our in vitro assays using rabbit fast skeletal muscle myosin. This was the myosin type that yielded the greatest observed sliding velocity of 4.6 μm/s. These values for α and β resulted in the magnitudes of some transition rates being larger than in the analysis of Pate and Cooke (1989), reflecting the increased temperature (30°C) for the present experiments. Variations in α and β, which provide fits to fit the mixture data in the presence of other myosin types, are considered in the Discussion. In model simulations of actively cycling smooth muscle and platelet myosins, 100% of the myosin cross-bridges were assumed to be phosphorylated.

Simulations followed the stochastic protocols employed by Brokaw (1976) with only slight modifications (Pate and Cooke, 1991). All simulations used an ensemble of 100 cross-bridges, with preassigned fractions of the possible myosin types. Sliding velocity for a given simulation was determined as the mean over a simulated 2.0-s time period, after an initial 1.5-s time period that allowed any initial transients to dissipate; δt was typically 0.05 ms. Values were then averaged over 5–10 distinct simulations (larger values for slower translation rates). The standard error in the simulations was less than 5% of the simulated mean value, except at the very lowest velocity levels, where it was approximately 0.002 μm/s. Solid-line fits in the figures are least-squares fits to the simulated velocities. There is additional discussion of the modeling protocols in Pate and Cooke (1991).

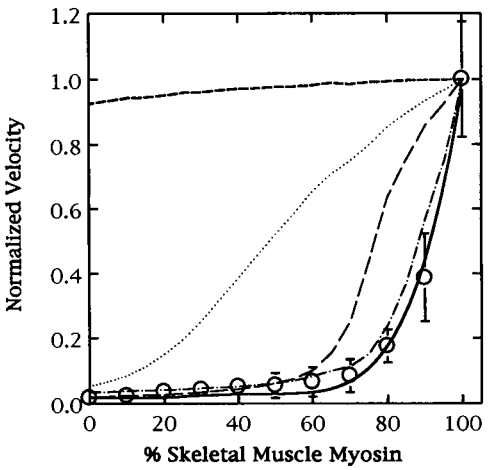

FIGURE 2 Sliding velocity for mixtures of rabbit fast skeletal and phosphorylated platelet nonmuscle myosin as a function of the percentage of fast myosin type. The left end of the horizontal axis corresponds to 100% platelet myosin type, the right end to 100% fast myosin type. The vertical axis gives the sliding velocity normalized with respect to the value obtained with 100% fast myosin type (4.5 μm/s). Phosphorylated platelet myosin moved at 0.08 μm/s. Data are mean ± SD. The long-dashed line is the fit to the data obtained by decreasing R_{12}, R_{23}, and R_{31} for platelet myosin by a factor of 56 from the values used for fast myosin in Eq. 2. The short-dashed, dotted, and dash-dot lines are obtained by sequentially decreasing only R_{12}, R_{23}, or R_{31} by a factor of 56, respectively, while keeping the other two kinetic parameters at the values for fast myosin. The solid line is the model fit as described in the text and Table 1, with $\alpha = 1$, $\beta = 1$ for fast myosin and $\alpha = 0.009$, $\beta = 1$ for platelet myosin.

RESULTS

Mixtures of actively cycling myosins with different translation rates

We have investigated seven pairwise mixings of actively cycling skeletal, smooth, cardiac, and platelet myosins. The differing myosins exhibit a wide range of in vitro sliding velocities (Table 1). Fig. 2 shows the results from mixing rabbit fast skeletal muscle myosin with phosphorylated, human platelet myosin. Fast skeletal muscle myosin alone translocated actin filaments with a mean velocity of 4.5 μm/s, whereas phosphorylated platelet myosin translocated filaments with a velocity of only 0.082 μm/s, ~50 times slower. The interesting observation was that the sliding velocity of the mixture did not increase linearly with an increasing fraction of the more rapidly translating myosin, as might be initially expected. Instead, the more slowly cycling platelet muscle myosin exerted a dominant effect on the velocity of actin filament sliding. As is evident in Fig. 2, when the amount of phosphorylated platelet myosin in a mixture of the two myosin types was 75% or greater, the velocity was very similar to that produced by phosphorylated platelet muscle myosin alone. A 50% decrease in velocity was obtained when only 8% of the myosin mixture was phosphorylated platelet myosin. One goal of this study is to understand the characteristics of the velocities of mixtures of myosins in terms of current chemomechanical models for cross-bridge kinetics. In this regard, the curve fits in Fig. 2 are from model analyses, as described in the Discussion.

Phosphorylated smooth muscle myosin moved actin filaments at a rate of 0.67 μm/s under these conditions. Although the data continued to exhibit similar concavity, the smaller, approximately sixfold difference in velocities, resulted in a less pronounced effect of the slowly cycling myosin on the velocity of fast skeletal muscle myosin (Fig. 3). The mixture sliding velocity was that of the slowly cycling form for a mixture containing 40% or more of the slowly cycling myosin type. A 50% reduction in overall velocity now required 25% of the myosin to be the more

TABLE 1 Experimentally observed, mean translation velocities for myosin types used in this study, along with values for α and β used in Eq. 2 to fit the velocity data in the mixing experiments for the solid lines in Figs. 2–10

Myosin type	Velocity (μm/s)	α	β
Fast skeletal (rabbit)	4.60	1.00	1.00
Fast skeletal (rat)	4.00	1.00	0.77
Phosphorylated gizzard	0.67	1.00	0.080
Phosphorylated platelet	0.082	1.00	0.009
Cardiac V1 (bovine)	1.65	1.00	0.24
Cardiac V3 (bovine)	0.53	1.00	0.065
Dephosphorylated gizzard	0.034	0.0017	0.076
Dephosphorylated platelet	0.0076	0.0004	0.009

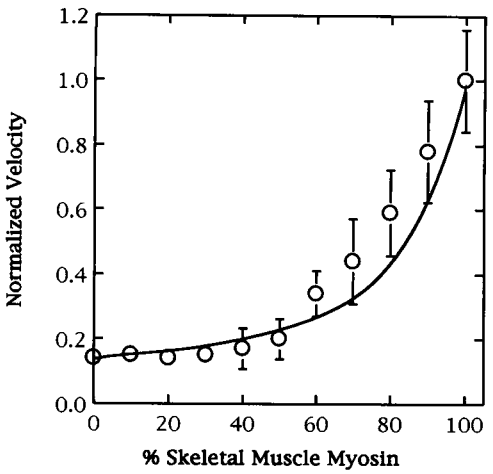

FIGURE 3 Sliding velocity for mixtures of rabbit fast skeletal and phosphorylated gizzard smooth muscle myosin as a function of the percentage of fast myosin type. Sliding velocity is normalized with respect to the value obtained with 100% fast myosin type (4.7 μm/s). The phosphorylated smooth muscle myosin moved at a velocity of 0.67 μm/s. Data are as in Fig. 2. The solid line is the model fit as described in the text and Table 1.

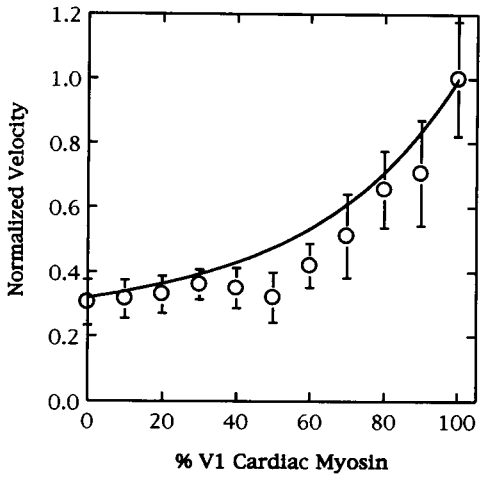

FIGURE 4 Sliding velocity for mixtures of V1 and V3 cardiac myosins. The data are as in Fig. 2, with velocities normalized with respect to that obtained with 100% V1 (1.7 μm/s). The solid line is the model fit as described in the text and Table 1.

slowly cycling form. Data similar to that in Figs. 2 and 3 were obtained by Warshaw et al. (1990) using the same assay, and by Sellers et al. (1985) using the *Nitella*-dependent in vitro motility assay. Larsson and Moss (1993) have likewise observed a similar behavior for maximum shortening velocity in permeabilized human quadriceps muscle as a function of slow myosin isoform. The solid line is the result of computer simulation, as subsequently discussed.

Cardiac myosin heavy chain exists as isoforms encoded by two different genes (α and β). These heavy chain isoforms can combine to form V1 myosin, which is an α-α homodimer; V2 myosin, an α-β heterodimer; and V3, a β-β homodimer (Hoh et al., 1993). The V3 myosin isoform is expressed in bovine ventricles, whereas the V1 isoform is expressed in bovine atria. Pure ventricular V3 myosin translocated actin filaments at a velocity of 0.51 μm/s, whereas atrial V1 myosin translocated at a velocity of 1.70 μm/s. Here the factor of 3 difference in translation velocities of the two myosin types was not as great as in Figs. 2 and 3. When these two myosins were mixed, we again found that the more slowly cycling V3 isoform dominated the velocity of the mixture (Fig. 4), although the effect was less pronounced than in Figs. 2 and 3. Similarly, each of these cardiac myosins were individually mixed with rat fast skeletal muscle myosin (Figs. 5 and 6). In both cases the more slowly migrating myosin dominated the rates of actin filament sliding, as evidenced by the upwardly concave curves. Finally, Fig. 7 shows results from mixing phosphorylated platelet myosin with phosphorylated smooth muscle myosin. Topologically similar results were again obtained, with the fivefold more slowly cycling platelet myosin dominating the velocity of the mixture. Model fits are also shown.

Mixtures of cycling and noncycling myosins

Unphosphorylated smooth muscle and unphosphorylated nonmuscle myosins bind to actin filaments in the presence of ATP but do not support movement (Warshaw et al., 1990; Sellers, 1985). It has been proposed that under these conditions, the myosin cross-bridges are in a weakly bound state (Sellers, 1985). Fig. 8 shows the results from mixtures of unphosphorylated and phosphorylated gizzard muscle myosin. As is evident, increasing proportions of unphosphorylated smooth muscle myosin slowed the movement of actin filaments when mixed with actively cycling myosins. Comparison with Figs. 2–7, however, shows that a significantly higher level of noncycling myosin was required to achieve the level of filament velocity attenuation that could

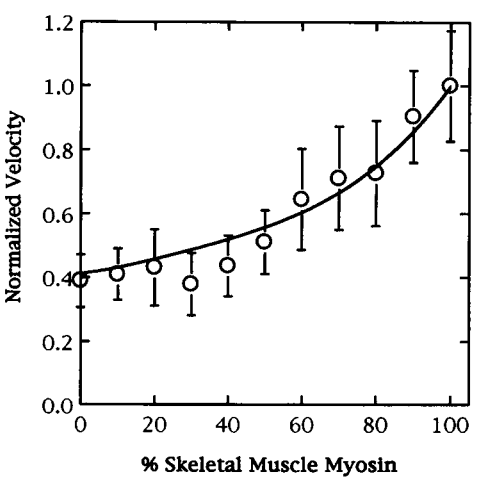

FIGURE 5 Sliding velocity for mixtures of fast skeletal muscle myosin and V1 cardiac myosin. The data are as in Fig. 2, with velocities normalized with respect to that obtained with 100% fast skeletal muscle myosin (4.1 μm/s). The solid line is the model fit as described in the text and Table 1.

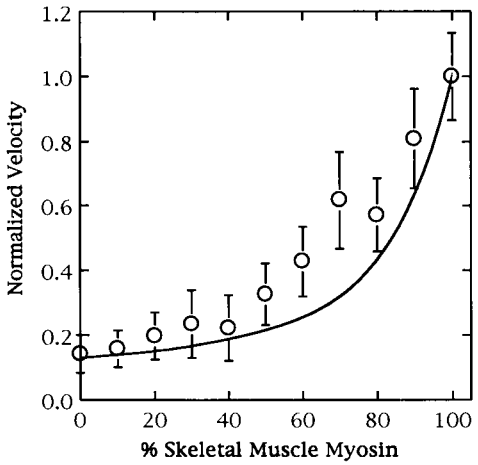

FIGURE 6 Sliding velocity for mixtures of fast skeletal muscle myosin and V3 cardiac myosin. The data are as in Fig. 2, with velocities normalized with respect to that obtained with 100% fast skeletal muscle myosin (3.9 μm/s). The solid line is the model fit as described in the text and Table 1.

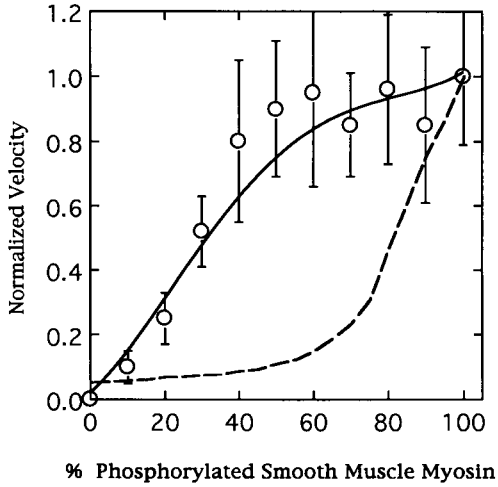

FIGURE 8 Sliding velocity for mixtures of actively cycling, phosphorylated smooth muscle myosin and noncycling, unphosphorylated smooth muscle myosin. The data are as in Fig. 2, with velocities normalized with respect to that obtained with 100% phosphorylated myosin (0.63 μm/s). The dashed line is obtained by decreasing all rate functions (R_{12}, R_{23}, and R_{31}) by a factor of 19, and clearly provides a poor fit to the data. The data are the average of two experiments, with the solid line giving the model fit as described in the text and Table 1.

be obtained when only a small level of actively but more slowly cycling myosin was mixed with more rapidly cycling myosin. Indeed, Fig. 8 shows that significant velocity reduction did not occur until >60% of the total myosin was of the unphosphorylated, noncycling species. Similar data have been obtained by mixing phosphorylated and unphosphorylated smooth muscle myosin (Sellers et al., 1985; Warshaw et al., 1990). Fig. 9 shows similar results for mixtures of phosphorylated and unphosphorylated platelet myosin. When unphosphorylated smooth muscle myosin was mixed with rapidly cycling skeletal muscle myosin, a nearly linear curve was obtained (Fig. 10). Thus noncycling myosin exerts a proportionally more dominant effect on the movement of the rapidly cycling skeletal myosin than it does on the more slowly cycling smooth muscle myosin. The continuous curve represents a model prediction, as described in the Discussion. The crucial observation, however, is that in all cases it is clear that the shape of the velocity curve for the mixture of cycling and noncycling myosins (Figs. 8–10) is distinctly different from that which

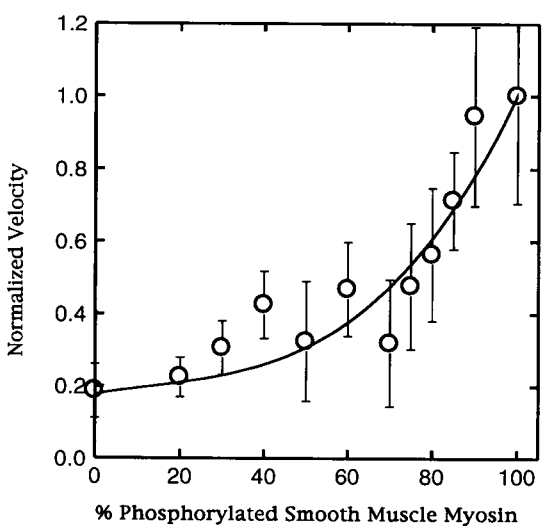

FIGURE 7 Sliding velocity for mixtures of phosphorylated gizzard smooth muscle myosin and phosphorylated platelet nonmuscle myosin. The data are as in Fig. 2, with velocities normalized with respect to that obtained with 100% phosphorylated gizzard smooth muscle myosin (0.61 μm/s). The sliding velocity of the 100% phosphorylated platelet myosin in this experiment was 0.113 μm/s. The solid line is the model fit as described in the text and Table 1.

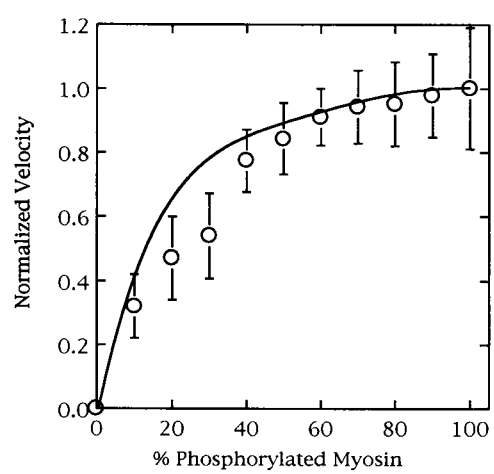

FIGURE 9 Sliding velocity for mixtures of actively cycling, phosphorylated platelet and noncycling, unphosphorylated platelet myosin. The data are as in Fig. 2, with sliding velocity normalized with respect to that obtained with 100% phosphorylated myosin (0.084 μm/s). The solid line is the model fit as described in the Discussion and Table 1.

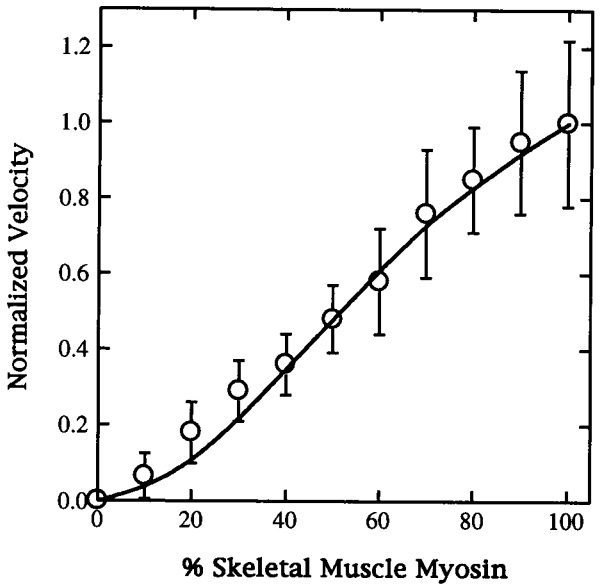

FIGURE 10 Sliding velocity for mixtures of actively cycling skeletal muscle myosin and noncycling human platelet myosin. The data are the average of two experiments. The solid line is the model fit as described in the text and Table 1.

we obtain for mixtures of rapidly and slowly cycling myosins (Figs. 2–7).

DISCUSSION

Myosins from different tissues and species each exhibit a characteristic rate of actin filament sliding in the in vitro motility assay. Normally in this assay, the viscous load on the actin filament is significantly less than the force produced by a cross-bridge, and thus the rate of sliding over any given myosin type is at the maximum value for the particular ionic conditions. We have examined the velocity of actin filament sliding over surfaces coated with mixtures of myosin types that individually exhibited different rates of filament translation. We also studied mixtures of cycling myosins and noncycling, unphosphorylated smooth and nonmuscle myosin. We found that the presence of fractions of noncycling and slowly cycling myosins altered the relative translation velocity generated by a more rapidly cycling myosin in a highly nonlinear fashion with respect to the concentration of the slowly cycling myosin. Furthermore, mixtures of slowly cycling and noncycling myosins with rapidly cycling myosins resulted in different shapes of the plot of aggregate mixture velocity.

Similar observations have previously been reported by Sellers et al. (1985) and by Harris et al. (1994). The latter authors considered extrapolations of steady-state, phenomenological, Hill, muscle force-velocity relationships into the negative force region for actively cycling cross-bridges, and postulated topologically similar, resistive force behavior for noncycling, unphosphorylated cross-bridges. Proportionally weighted combinations of the values for maximum shortening velocity (unloaded sliding) yielded relationships similar to those experimentally observed. However, the relationships between the intermediate chemomechanical states in the working cross-bridge cycle and the phenomenological Hill fit remain poorly understood. In the present study we have considered an expanded repertoire of myosin types. The increased data base in the present study has allowed us to more extensively test the degree to which current hypotheses regarding cross-bridge function are compatible with the highly diverse, nonlinear responses of mixtures of cross-bridge types. In particular, we have now been able to consider the experimental data in terms of chemomechanical models for the fundamental steps in the cross-bridge cycle. These models are based upon the hypothesis, originally due to Huxley (1957), that attached cross-bridges function as elastic elements.

Active shortening in contracting muscle, or filament sliding in the more recently developed in vitro assay protocols, is generally understood to result from a cyclic interaction between myosin cross-bridges with actin-binding sites. Considerable experimental evidence has pointed to the following basic cycle (reviewed in Cooke, 1986; Goldman, 1993; Brenner, 1990). Initial cross-bridge attachment is in a weakly bound, low-force-producing state in which either ATP or the hydrolysis products (ADP, P_i) are bound to myosin. There is a subsequent transition to a high-force, strongly bound state. In both skeletal and smooth muscle, this transition appears to be associated with phosphate release from the weakly bound state. During active shortening, the strongly bound cross-bridge then executes a power stroke, resulting in actin filament sliding. When continued attachment of the strained cross-bridge to the actin filament would retard useful motion, ADP is released; ATP binds to myosin, dissociating the cross-bridge from the actin filament; and the cycle can begin again.

This envisioned pathway for actively cycling cross-bridges is mapped by the solid arrows in Fig. 1, which shows free energy as a function of the spatial relationship x between a cross-bridge and an actin-binding site (Eq. 2, Materials and Methods). With reference to the rate functions given in Eq. 3, binding sites enter from the right in the model. Initial attachment is in the weakly bound state 2. With continued sliding, it becomes both energetically and kinetically favorable for an attached cross-bridge to make the transition to the strongly bound state 3 when $x < 7$ nm. During the power stroke ($0 < x < 7$ nm), mechanical work is then produced at the expense of chemical free energy. For $x < 0$ nm, continued attachment of the linearly elastic cross-bridge results in a counterproductive, resistive force to further actin filament sliding. R_{31} is assumed to become large and results in cross-bridge detachment to state 1. The cycle can then begin again.

On the other hand, if the transition rate between states 1 and 2 is sufficiently small, the state 1 to state 2 transition does not occur (even though it is energetically favorable). This has been suggested to be the case with noncycling, unphosphorylated myosins, where the weak-to-strong tran-

sition rate, R_{12}, is dramatically reduced. Cross-bridges can then detach only as active sliding decreases the value of the spatial parameter, ultimately resulting in the free energy of the attached state being above that of the detached state (Fig. 1, *open arrows*). We shall continue to use the term "actively cycling" to refer to myosins that make the transition into the strongly bound state and "noncycling" to refer to myosins that are inhibited at this step (unphosphorylated smooth and platelet myosins).

Thus as will be shown, the data involving sliding velocities generated by mixtures of different myosins allow us to test the implications of modifications at two pivotal points in the contractile cycle: 1) the weak-to-strong transition (inhibited in unphosphorylated, smooth muscle and platelet myosin) and 2) detachment of retarding, negatively strained cross-bridges.

Mixtures of actively cycling cross-bridges

The parameters used to quantitate the above chemomechanical cycle are detailed in Materials and Methods. Equation 2, with $\alpha = \beta = 1$, provides the best fit to the sliding velocity of rabbit fast skeletal muscle, the myosin that translocated filaments most rapidly in our assays. Assuming that our fundamental hypotheses regarding the nature of the contractile cycle are relevant to all of the myosin types used in these assays, we may now ask how modifications of the individual kinetic parameters of a specific myosin type affect its predicted motility rate and its behavior in a mixture.

There is some tendency for more slowly cycling myosins to have kinetic rates that are slower at multiple points in the chemomechanical cycle. Although this is clearly not an obligatory requirement for myosins to cycle more slowly (see, for example, tables 10–12 in Sellers and Goodson, 1995), it nonetheless provides a useful starting point for quantitative analysis. In the data of Fig. 2, phosphorylated platelet myosin translocated filaments at a rate that was 56-fold slower than fast skeletal muscle. The long-dashed line in Fig. 2 shows a model in which skeletal muscle myosin was mixed with a hypothetical myosin in which all of the rate transitions were reduced by a factor of 56 as a model for phosphorylated platelet myosin. The long-dashed line in Fig. 2 shows that a reasonable, although hardly compelling, fit to the experimental mixing data can be obtained by using these fast skeletal and platelet rate functions.

We simultaneously modified three rates (attachment, weak-to-strong state, and detachment) to generate the dashed fit in Fig. 2. It is now useful to determine the degree to which each of the three modifications individually contributes to the final dashed line fit of the mixing data. To address this issue, Fig. 2 also shows three additional mixing simulations. These were performed using the original model parameters for fast skeletal myosin as above, but sequentially modifying one of the three rates by a factor of 56, while leaving the other two rates unchanged. Thus the upper curve (*short dashes*) shows the mixing simulation when only the attachment rate (R_{12}) is decreased, leaving the other two transition rates unchanged (R_{23} and R_{31}). As is evident, a decrease in the attachment rate has little effect on the sliding velocity of the mixture, because the modeled velocity of even 100% phosphorylated platelet myosin is only 5% less than that of 100% fast skeletal myosin. Similarly, the dotted curve in Fig. 2 shows the result obtained when only the transition rate from the weakly bound pre-power-stroke state to the strongly bound power-stroke state is decreased (R_{23}). The final dash-dot curve shows the result obtained when only the detachment rate in the drag stroke (R_{31}) is decreased. This latter fit clearly provides a much more reasonable fit to the experimental data.

The drag stroke detachment rate (R_{31}) has previously been proposed to be rate limiting, potentially associated with ADP release (Siemenkowski et al., 1985) at physiological substrate concentrations. Likewise, as has previously been suggested on both theoretical (Pate and Cooke, 1989) and experimental grounds (Millar and Homsher, 1992), a sufficiently slow weak-to-strong transition rate can be partly rate limiting to the overall cycle rate. These observations are again demonstrated by the decreases in sliding velocity obtained for 100% phosphorylated platelet myosin when R_{23} and R_{31} were decreased. The important observation, and one of our fundamental points, however, is that with regard to understanding the myosin chemomechanical cycle, the experimental data from the mixing plots provide considerably more information than just the sliding velocity generated by 100% of a given myosin type. As is evident from Figs. 2–7, irrespective of the sliding velocities of the myosins in isolation, we observe a distinct, upward concavity associated with mixture data from actively cycling cross-bridges. Slowly cycling myosins dominate rapidly cycling myosins. For example, compare the mixing experiments involving phosphorylated smooth muscle myosin (Figs. 3 and 7). Regardless of whether phosphorylated smooth muscle myosin is the faster myosin (Fig. 7) or the slower myosin (Fig. 3), both plots are upwardly concave. From the dash-dot line in Fig. 2, the dominance by the slower cycling myosin is clearly associated primarily with differences in the drag-stroke detachment rates. We feel it is important to reemphasize one of the fundamental constraints in the approach we took to fitting the data. For all myosin types, the model parameters (α and β) were chosen to fit the sliding velocities of specific, given myosin types in isolation. The fact that the proportional mixture data are then subsequently fit so well by our analysis provides additional confidence in our approach.

Analysis of the strongly bound state via a simplified model

Can we now better understand how differences in drag-stroke detachment rates from the strongly bound state influence the shape of the data obtained from the mixture

experiments? More detailed analysis of the model for actively cycling myosins indicated that more than 85% of the total sum of the absolute values of the force of the attached cross-bridges resulted from strongly bound cross-bridges. In other words, to a first approximation in balancing the forces that determine sliding velocity, the weakly bound state may be ignored. In the Appendix, we take advantage of this model simplification, omitting the second-order force contribution from the weakly attached state and consider a simplified, two-state chemomechanical model involving only a single, strongly bound, attached state. The model is based upon the original cross-bridge analysis by A. F. Huxley (1957) and has the additional advantage of being analytically tractable. To fix notation, assume that the rapidly and slowly cycling myosin types have drag-stroke detachment rates g_r and g_s, respectively. Here $g_r > g_s$, with increasing relative velocity differences increasing the strength of the inequality. In the Appendix, we show that if a small fraction, σ, of slowly cycling myosin is added to 100% rapidly cycling myosin, the normalized mixture velocity will be expected to initially decrease with a slope approximately proportional to $\sigma(g_r/g_s)^2$. Conversely, if a small fraction, ρ, of rapidly cycling myosin is added to 100% slowly cycling myosins, the normalized mixture velocity initially increases with only a modest slope approximately proportional to $\rho/2$. This is, of course, precisely the behavior we see in our mixing experiments involving actively cycling cross-bridges. Only small proportions of a slowly translating myosin are necessary to slow the velocity of a rapidly translating myosin; a substantial fraction of a rapidly cycling myosin is required before there is any significant increase in the normalized velocity of a mixture dominated by a slowly cycling myosin. Furthermore, as is evident from comparing the shapes of the mixture velocity plots in Figs. 2–7, the effect of adding slowly cycling myosins to rapidly cycling myosins becomes increasingly accentuated as the relative velocity difference between the two myosin types increases. This is the behavior to be expected, if even small differences in drag-stroke detachment rates are amplified, not linearly, but quadratically, as implied by the $(g_r/g_s)^2$ dependence discussed above and in the Appendix.

As noted, our modeling suggests that the chemomechanical properties of mixtures of actively cycling myosins are dominated by the magnitude of the drag-stroke detachment after the power stroke (R_{31}). There has as yet been no complete characterization of the degree to which other transition rates differ among the varying myosin types. Thus we have also endeavored to determine if a reasonable fit to the aggregate mixture sliding velocity data can be obtained while holding R_{23} constant in Eq. 2 by using the value $\alpha = 1$ from fast skeletal muscle, and while varying only R_{31} via the multiplicative parameter β. The fits obtained are given by the solid lines in Figs. 2–7. Experimentally measured values for the sliding velocities of the different myosin types, and values of β used for the fits, are summarized in Table 1. We note that the value of β associated with platelet myosin in Table 1 is different by less than a factor of 2 from that used in Fig. 2 to account for the 56-fold difference in sliding velocities when all kinetic steps were reduced. As anticipated, smaller sliding velocities are associated with smaller values of β. It should be noted that with R_{23} fixed, the sliding velocity is only approximately proportional to β. The appendix of Pate and Cooke (1991) previously shown that this results from a balancing of transition rates and elastic forces in different kinetic regimes.

Mixtures of cycling and noncycling cross-bridges

The second type of experiment involved filament sliding velocities in the presence of varying fractions of noncycling, unphosphorylated smooth and platelet myosin. Biochemical evidence has suggested that the rate-limiting step in the ATPase kinetic cycle for these myosins is at the weakly to stongly bound transition (Sellers, 1985). Phosphorylation of smooth muscle HMM increased the weak-to-strong transition rate by a factor of about 1000 without significantly affecting other transition rates in the hydrolysis cycle (Sellers, 1985; Greene and Sellers, 1987). These noncycling myosins were mixed with actively cycling myosins for which the kinetic step limiting the rate of actin filament sliding is cross-bridge detachment in the drag-stroke region of the cycle. As is evident in Figs. 8–10, these noncycling myosins also decreased the sliding velocity generated by the cycling myosins. The noncycling myosins presented less mechanical drag than was exhibited when a slowly cycling myosin was mixed with a rapidly cycling myosin, however. Similar data have been obtained by Warshaw et al. (1990). A noncycling analog of the weakly bound state of myosin could be produced by chemical modification of skeletal muscle myosin with *N,N′-p*-phenylenedimaleimide (pPDM) (Chalovich et al., 1983). Warshaw et al. (1990) showed that pPDM-modified skeletal muscle could slow the rate of actin filament sliding when mixed with actively cycling rabbit skeletal muscle myosin or phosphorylated smooth muscle myosin. The extent of inhibition of the rate of sliding was similar to that obtained when these actively cycling myosins were mixed with unphosphorylated smooth muscle myosin.

Modeling analyses can provide insights into mechanisms by which these noncycling cross-bridges can provide drag. Attempts to model the effects of unphosphorylated myosins on sliding velocity by simultaneously altering all kinetic rate constants again proved unsuccessful, resulting in plots of velocity versus the fraction of actively cycling cross-bridges that were concave up (Fig. 8, *dashed curve*). Instead, for the present modeling studies involving unphosphorylated myosins, the cross-bridge attachment rate, R_{12}, and the parameter determining the off-rate in the dragstroke region $x < 0$ (R_{31}), were taken as identical to those established in the simulations for the phosphorylated forms of the myosins as given in Table 1. Then, consistent with the biochemical data, the weak-to-strong transition rate, R_{23}, was adjusted by varying the parameter α. Reasonable fits

were obtained with $\alpha = 0.0017$ (smooth muscle) and $\alpha = 0.0004$ (platelet). Both are different by only a factor of ~2 from the factor 0.001 suggested by the solution biochemistry data derived from kinetic studies of gizzard smooth muscle myosin (Sellers, 1985).

The data in Figs. 8 and 9 result from varying fractions of phosphorylated and unphosphorylated myosins of the same type, with an increasing fraction of weakly bound cross-bridges as the proportion of dephosphorylated myosin increases. Fig. 1 provides insight into the reasons the weakly bound cross-bridges can retard sliding velocity. Both cycling and noncycling cross-bridges attach in state 2 for $x > 7$ nm. For $x < 7$ nm, the transition to the strongly bound state is now energetically favorable (*solid arrows*; the pathway followed by the actively cycling cross-bridges). However, with R_{23} taken to be small (α small) for the unphosphorylated cross-bridge fraction, extremely few unphosphorylated cross-bridges make this transition. Instead they must be "mechanically detached" as continued sliding pulls them into the region where the free energy of the detached state 1 is lower than that of the attached state (*open arrows*). Cross-bridges in state 2 with spatial coordinate $x > 7$ nm produce positive forces; cross-bridges in state 2 with $x < 7$ nm produce negative forces. Thus a distribution of cross-bridges in the weakly bound state 2, which is symmetrical with respect to $x = 7$ (i.e., symmetrical with respect to the free energy profile of state 2), will produce no net force and hence no net drag. However, with the rate functions used, cross-bridges that attach at values of $x > 7$ nm are carried to lower values of x via filament sliding. Thus an asymmetrical distribution is developed, with a greater number of cross-bridges in state 2 with $x < 7$ nm, and hence a resistive force is generated by weakly bound cross-bridges.

The inhibition requires the rate functions to be in the proper range. For example, consider the case in which the attachment rate R_{12} is increased everywhere by a multiplicative factor of 1000. With this more rapid transition rate, resistive cross-bridges in state 2 are able to more rapidly equilibrate with respect to free energy into the detached state 1. Simulations show that in this case the decrease in velocity with increasing proportions of unphosphorylated cross-bridges is dramatically reduced (only a 12% reduction at 80% unphosphorylated cross-bridges instead of the 60% observed in Fig. 8), because any cross-bridge force asymmetry that develops because of filament sliding is dissipated in the free energy equilibration between attached and detached states. The important observation is that the precise analytical form of R_{12} is not critical to the model analysis. The crucial aspect is that the rate functions allow a spatial cross-bridge distribution in state 2 that is asymmetrical with respect to $x = 7$ nm. The degree to which this occurs then determines the fraction of noncycling bridges that are required for any significant reduction in velocity.

The ability of weakly bound cross-bridges to produce a resistive drag on filament sliding velocity is a property not generally associated with these cross-bridges. This view derives from the original analyses investigating the mechanics of weakly bound cross-bridges in relaxed rabbit psoas fibers (Brenner et al., 1982; Schoenberg, 1988). The data from these studies clearly demonstrated that at realistic sliding velocities, the mechanical drag that could be produced by relaxed, weakly bound cross-bridges was minimal. Subsequent studies with active fibers, however, suggest to the contrary the possibility that weakly attached states can present a load on maximum shortening velocity. Phosphate release in actively contracting fibers is thought to be involved in the transition from the weakly to strongly bound cross-bridge states, with increasing $[P_i]$ resulting in a shift of cross-bridges into weakly attached states. Phosphate analogs such as orthovanadate (V_i) or aluminum metallofluoride complexes bind to the A·M·ADP state, stabilizing the cross-bridges in a state thought to resemble the weakly bound, pre-power-stroke state (Herzig et al., 1981; Dantzig and Goldman, 1986; Chase et al., 1993). Increasing concentrations of these analogs increase the proportion of weakly bound cross-bridges and have been shown to decrease shortening velocity in chemically skinned muscle preparations (Herzig et al., 1981; Chase et al., 1993). Additional indications that weakly bound states can provide a resistive drag to sliding is provided by studies on the mechanics of skinned muscle fibers using nonnucleoside triphosphate substrates. Here, observed variation in sliding velocity with variation in nonnucleoside triphosphate substrate has been shown to be compatible with increasing resistive drag from weakly bound cross-bridges (Wang et al., 1993a). The analysis of the data in the present work provides additional support for this new, expanded role of weakly bound cross-bridge states in the modulation of actomyosin chemomechanics.

In contrast to the experimental observations, we note that in Figs. 8–10, the simulated velocity at 100% noncycling myosin is close to but not equal to zero. This is due to the fact that a small but nonzero value for R_{12} results in the modeled cross-bridges actually continuing to cycle very slowly. The effect is most noticeable in Fig. 9 (phosphorylated and unphosphorylated platelet myosins) where the simulated proportional velocity at 100% unphosphorylated myosin type is largest. Much better fits are obtained if R_{12} is reduced by an additional factor of 3 for both phosphorylated and unphosphorylated platelet myosin. The precise magnitude of this transition rate has not been determined for platelet myosin. Additionally, other non-cross-bridge-dependent mechanical factors may become experimentally important at the extremely small simulated velocities obtained for 100% unphosphorylated myosin. These may have an additional effect on experimentally observed translation velocities.

Phosphorylation of the 20-kDa light chain of myosin initiates smooth muscle contraction, although it is clear from a number of tissues that submaximum extents of phosphorylation are usually obtained (i.e., less than 1 mol of P_i incorporated per 20-kDa light chain of myosin) and that there is not a linear relationship between peak isometric force and extent of light chain phosphorylation (Hai and Murphy, 1989). Unloaded shortening velocity does corre-

late with the extent of phosphorylation (Dillon et al., 1981), and it is possible that this correlation may be due to the weakly bound, unphosphorylated myosins acting as a load that acts to slow the translocation of actin by the actively cycling phosphorylated cross-bridges.

Relationship to other studies

Other experimental studies have also found upwardly concave relative velocity plots when actively cycling myosins were mixed. However, the shape of the mixing curve in Fig. 5 (fast skeletal muscle myosin versus bovine atrial V1 myosin) is different from that reported by Harris et al. (1994) for chicken fast muscle myosin and rat V1 cardiac myosin. In their study, increasing fractions of actively cycling, fast skeletal muscle resulted in a relative velocity plot that was concave downward with increasing proportion of the rapidly cycling myosin. In Fig. 5 our plot is concave upward. This difference has not been reconciled. It could be due to species differences, or differences in the ionic conditions of the assays.

As is evident from Figs. 2–10, we have been able to obtain reasonable fits to all our accumulated data by using a single cross-bridge model involving only multiplicative modifications of single rate functions for differing myosin types. This approach was motivated by our observation that kinetic rate function modifications at two distinct points in the chemomechanical cycle appear to have very distinct effects on the shape of the mixture velocity plots. Differences other than simply kinetic rates have been suggested for different myosin types, however. It is important to consider the implications of these differences in the context of the model.

Intact or skinned smooth muscle preparations produce more force per cross-bridge than do skeletal muscle preparations. On the assumption that this enhanced tension is a result of differences in the properties of the cross-bridges themselves, it could be the result of a higher unitary force per cross-bridge (e.g., elastic force constant) or of an increased attached duty cycle for smooth muscle myosin. Using in vitro, microneedle assays, VanBuren et al. (1993) have suggested that smooth muscle myosin does indeed produce a higher force per cross-bridge when compared to fast skeletal myosin. Motivated by theoretical considerations from phenomenological Hill fits (Harris et al., 1994), VanBuren et al. (1995) performed similar in vitro assays, which suggested additional differences in the force per cross-bridge among V1 and V3 cardiac myosins. However, in both of these cases, an interpretative problem arises from the fact that the actual forces per cross-bridge experimentally measured for smooth, cardiac, and skeletal myosins were a full order of magnitude lower than the value that has been observed for single fast skeletal muscle myosin molecules using optical trap protocols. Following this line of inquiry, Guilford et al. (1996) have recently disputed the claim of different elastic force constants. Their optical trap experiments on single smooth muscle myosin molecules indicate a unitary cross-bridge force of 3–4 pN, a value comparable to that obtained for fast skeletal preparations. This result would imply that the difference is in the cross-bridge duty cycle.

The cross-bridge duty cycle is directly related to cross-bridge kinetics. The slower mechanical transients following rapid length changes in smooth muscle preparations as compared to those in fast skeletal preparations (Yamakawa et al., 1990) could be interpreted to imply an increased proportional time a cross-bridge is attached to actin and thus an increased duty cycle. However, in the absence of sarcomere length servo control, the significant series elastic component present in smooth myosin can dramatically slow tension transients relative to the underlying biochemical kinetics (Brenner and Eisenberg, 1986; Luo et al., 1993), making correlations between transient mechanics and biochemistry difficult to rigorously establish. Also arguing against different duty cycles are the in vitro assay data of Harris and Warshaw (1993b), suggesting instead that fast skeletal and smooth muscle myosins have approximately the same duty cycle.

Additional experimental data will clearly be required to understand these differences. It is important to observe, however, that models of the cross-bridge cycle indicate that different experimental protocols could yield different estimates of the duty cycle in actively cycling cross-bridges. Since the original analysis by Huxley (1957), it has been recognized that the duty cycle in the isometric state is determined solely by kinetic rates in the power stroke; drag-stroke rates become involved only under conditions of unloaded shortening. Differing relative tunings of power-stroke and drag-stroke rates in myosins that serve different physiological functions could result in optical trap (i.e., isometric) protocols and in vitro sliding assays, giving different estimates of the duty cycle.

In light of our experimental protocol, we have concentrated on the interpretation of the duty cycle when filament sliding effects are involved. Our analysis does make predictions regarding the chemomechanical differences between myosins that were addressed in the previous paragraphs. We have made the simplest assumption that all cross-bridges have the same elastic force constant. As demonstrated in Eqs. A.2 and A.3, if the elastic force constant of the more slowly cycling myosin is greater than that of the more rapidly cycling myosin, the positive concavity that we observe will decrease. A sufficiently large difference in myosin cross-bridge elastic force constants between rat cardiac V1 myosin and fast chicken myosin could offer a potential resolution of the concavity differences in the observations of Harris et al. (1994) and our observations on mixtures of fast rabbit skeletal muscle myosin and bovine atrial V1 myosin.

Reducing all kinetic rates by an equal fraction to produce a more slowly cycling modeled myosin type will result in an unaltered, attached duty cycle. Transitions between states

will be less frequent, but the fraction of time per state will remain unchanged. This is consistent with the in vitro observation of Harris and Warshaw (1993b) that fast skeletal and smooth muscle myosins have approximately the same duty cycle. In our simplified analysis, we have altered only one transition rate. Does this assumption yield results that are compatible with these experimental data? For our model parameters, we determined the duty cycle from simulations of filament translation generated by a single myosin cross-bridge of a specific type. Representative values (mean ± SEM, five simulations of 200 s duration each) were 4.3 ± 0.05% (rabbit fast skeletal myosin), 5.0 ± 0.04% (cardiac V1 myosin), 7.2 ± 0.06% (phosphorylated gizzard myosin), and 24.5 ± 0.33% (phosphorylated platelet myosin). Duty cycles of approximately 5% have been reported previously by Uyeda et al. (1990) and by Harris and Warshaw (1993b) for fast skeletal and smooth muscle myosins.

Despite the fact that we have altered only one kinetic rate instead of all kinetic rates to model a more slowly cycling myosin, we still predict little variation in the cross-bridge duty cycle, except for the very slowest myosin type. It is easy to see why this occurs. Uyeda et al. (1990) initially observed that a low duty cycle requires the rate-limiting kinetic step to occur on the detached cross-bridge. This is indeed the case for the single cross-bridge duty cycle simulations reported here. Initial cross-bridge attachment is the rate-limiting step, except for the very smallest values of β in Eq. 2. The precise shapes of the rate functions employed are not crucial. Our crucial observation is that when initial cross-bridge attachment (or another transition rate other than drag-stroke detachment) is the rate-limiting step in the cross-bridge cycle, significant changes in sliding velocities can occur for ensembles of cross-bridges, with only minimal changes in the single cross-bridge duty cycle. Even for the extremely slowly cycling platelet myosin, the detachment rate at the end of the power stroke is 18 s^{-1}, still faster than the initial attachment rate in the single cross-bridge simulations. Hence for a ensemble of 100 cross-bridges, a >50-fold decrease in sliding velocity, relative to rabbit fast skeletal myosin, can correspond to a <6-fold decrease in the duty cycle. The duty cycle of platelet myosin has not been experimentally determined.

Subject to the above duty-cycle constraint, we reemphasize that our analysis does not preclude modifications of other kinetic rates in the myosin cycles. Indeed, as previously noted, we were able to obtain better fits to the phosphorylated versus dephosphorylated platelet myosin mixing experiments (Fig. 9) via an additional modification of the weak-to-strong transition rate. We have previously indicated the effects of reductions in the weak-to-strong and drag-stroke detachment rates. For the sake of completeness and with reference to Fig. 2, we note that less extensive simulations suggest that a further decrease in the initial attachment rate (R_{12}) enhances the downward concavity, which is weakly exhibited in Fig. 2.

An alternative explanation for our ability to obtain reasonable fits to the data for actively cycling myosins via modification at a single kinetic step is that there is a rough inverse relationship between sliding velocity and average isometric force (as experimentally measured in intact preparations) for skeletal, smooth, and cardiac muscle preparations. We fit our results by assuming that the sliding velocity of each actively cycling myosin type is determined solely by the detachment rate constant. Thus the slower the myosin, the slower the detachment rate constant will be. As shown, this has a dramatic effect on the resistive force a myosin produces when mixed with a faster myosin type. Thus our fit could simply be a result of the fortuitous inverse relationship between sliding velocity and isometric force for smooth muscle and the two cardiac muscle myosins. However, our simultaneous ability to also fit the data from the mixtures of the two cardiac myosins, and platelet myosin with both skeletal and smooth muscle myosins would argue against a simple fortuitous set of circumstances.

In summary, we have investigated the actin filament in vitro translation velocities generated by mixtures of a wide range of both cycling and noncycling myosin isoforms. The observed sliding velocities were highly nonlinear and of varying concavity with respect to the proportions of the myosin types. However, our analysis indicated that the data were compatible with current hypotheses regarding myosin cross-bridge function. We have been exceptionally surprised to find that very reasonable fits to all of our mixing data velocities (nine sets) can be obtained by proportional modifications in the transition rates between cross-bridge states at only two points in the cross-bridge cycle. Chemomechanical models based upon the original analysis of Huxley (1957) suggest that the experimentally observed behavior is to be expected if both actively cycling and noncycling cross-bridges can provide a resistive drag. The models indicate that a decrease in velocity of an actively cycling myosin resulting from increasing proportions of more slowly but still actively cycling cross-bridges results from a dramatic amplification of any difference in cross-bridge detachment rates in the drag-stroke region. Noncycling, weakly attached cross-bridges can likewise provide a drag if a spatially asymmetrical cross-bridge distribution is produced in the weakly bound state.

Different myosin types most certainly differ in kinetic rates and mechanical constants. Given the plethora of potentially pertinent parameter differences, we would appear to have identified two transitions that exert more than their fair share of influence on the nature of the mixture sliding plots. More importantly, however, the robust nature of our modeling approach (modifications of kinetic rates, cross-bridge constants, etc. are quite easily programmed) could make it a useful tool for understanding the influences of other chemomechanical differences between myosin types on in vitro assay experimental data as more extensive kinetic and mechanical parameter data bases become available.

APPENDIX

Our experimental data indicated that when actively cycling cross-bridges were mixed, only very small proportions of the more slowly cycling myosin type were required to significantly inhibit sliding velocity. Our purpose here is to provide analytical insight into how this highly nonlinear response can be expected from current hypotheses regarding cross-bridge function.

As noted in the text and demonstrated in Fig. 2, model sliding velocity is primarily determined by the drag-stroke detachment rate from the strongly bound state for mixtures involving only actively cycling cross-bridges. Thus for analysis, we limit ourselves to a simpler, two-state model (Pate et al., 1993), similar to that originally proposed by Huxley (1957). We assume only a single detached state and a single, attached, strongly bound, and force-producing state. Let all binding sites again enter from the right (as in Fig. 1). Assume cross-bridges attach at some arbitrary point, $x = h$, and traverse the powerstroke $h \geq x \geq 0$ in the direction of decreasing x as given by the solid arrows in Fig. 1. Assuming the cross-bridges are linearly elastic, with elastic force constant, κ, then to within a multiplicative constant dependent upon the total cross-bridge density, the positive force produced by the power-stroke cross-bridges will be $F_+ = \kappa h^2/2$. In the drag-stroke region, $x < 0$, let cross-bridges detach with rate constant g. Taking sliding velocity V as a positive quantity, the fraction n of attached cross-bridges in the drag stroke will decay exponentially as $n(x) = \exp[gx/V]$. The negative force produced by the drag-stroke cross-bridges is determined by integrating $n(x)\kappa x$ (cross-bridge fraction times force per cross-bridge) over the region $(-\infty, 0]$, obtaining $F_- = -\kappa V^2/g^2$ (again to within a density-dependent proportionality constant). As originally observed by Huxley, for unloaded shortening as in the in vitro assay experiment, V will be the velocity for which $F_+ + F_- = 0$ (i.e., no net force on the filament). Solving:

$$V = gh/\sqrt{2}. \tag{A.1}$$

In the three-state model, variation of the cross-bridge detachment rate parameter is equivalent to variation in the parameter g in our simplified, two-state model. Consider the case of a mixture of a fraction, σ, of slowly cycling cross-bridges (with detachment rate g_s in the drag-stroke region) and corresponding fraction $1 - \sigma$ of rapidly cycling cross-bridges (with detachment rate g_r). Then for unloaded sliding, V is again determined by a balance of positive and negative forces from each cross-bridge type, $F_{+s} + F_{+r} + F_{-s} + F_{-r} = 0$, where the subscripts r and s have been added to denote the contributions from the rapidly and slowly translating cross-bridges. We additionally allow for the possibility of different elastic force constants for the two myosin types, $\kappa_s = \eta\kappa_r$. Then as above,

$$\sigma[\tfrac{1}{2}\kappa_s h^2] + (1 - \sigma)[\tfrac{1}{2}\kappa_r h^2] - \sigma[\kappa_s V^2/g_s^2] - (1 - \sigma)[\kappa_r V^2/g_r^2] = 0.$$

Solving for the unloaded sliding velocity V,

$$V = \frac{g_r g_s h[1 + \sigma(\eta - 1)]^{1/2}}{2[(1 - \sigma)g_s^2 + \sigma\eta g_r^2]^{1/2}}. \tag{A.2}$$

This is more complex than the expression for V than when only a single myosin type is involved. However, several rearrangements of Eq. A.2 can help to bring the interplay of the various terms into focus. Consider first the case in which a very small fraction of the slowly translating myosin type is added to a population of the rapidly translating myosin type. Then we can take $\sigma \ll 1$, and expanding the right-hand side of Eq. A.2 in powers of σ yields (first two terms):

$$V = \{g_r h/\sqrt{2}\}\{1 - \sigma\eta[(g_r/g_s)^2 - 1]/2 \pm \ldots\}. \tag{A.3}$$

Conversely, consider the situation in which a fraction, $0 < \rho \leq 1$, of rapidly translating cross-bridges is added to a population consisting of 100% slowly translating cross-bridges. (Mathematically, this is equivalent to replacing the slow fraction, σ, with $1 - \rho$ in Eq. A.3.) Assuming again that the added fraction is small, $\rho \ll 1$, then an analysis as above yields (first two terms)

$$V = \{g_s h/\sqrt{2}\}\{1 + \rho\eta[1 - (g_s/g_r)^2]/2 \pm \ldots\}. \tag{A.4}$$

In Eq. A.3 (A.4), the first term in braces is the velocity produced by rapidly (slowly) cycling cross-bridges in the absence of any slowly (rapidly) cycling cross-bridges (see Eq. A.1). The second term in braces is the modification in the velocity as the fraction of the other cell type increases. We facilitate further discussion of the implications of Eq. A.3 by considering the data in Fig. 2. Here the 56-fold difference in sliding velocities between the fast skeletal and platelet myosin types is equivalent to $g_r \gg g_s$. Then Eq. A.3 indicates that addition of a small proportion of slowly cycling myosin to the fast myosin decreases the mixture velocity at a rate proportional to $[(g_r/g_s)^2 - 1]/2 \approx (g_r/g_s)^2/2$. In other words, any small difference in the ratio of the individual sliding velocities is amplified quadratically in the velocity decrease of the mixture. Thus as we observe in Figs. 2–6, the model likewise predicts a progressively less dramatic decrease in velocity when the differences in sliding velocities decrease.

Considering Eq. A.4, the term in the second set of braces gives the modification in the velocity as the fraction, ρ, of rapidly cycling cross-bridges increases. With $\rho = 1$ and $(g_s/g_r)^2 \ll 1$, as ρ increases, velocity increases, but now only linearly with a modest slope ≈ 0.5. For ρ increased to even 1 (100% rapidly translating myosins), the relationship implies a small initial velocity increased by only 50%. This value for ρ is, of course, outside of the range of validity of our approximation. Nonetheless, our conclusions are consistent with the data in Fig. 2. Very small fractions of slowly translating cross-bridges can dramatically decrease the translation velocity of rapidly translating cross-bridges; large fractions of rapidly cycling cross-bridges can be necessary to increase the velocity of slowly translating cross-bridges.

The above analyses assume small fractions of a cell type and are thus local in nature. Globally, we also note that the graph of V^2 (Eq. A.2) is a hyperbola. With $\eta = 1$, the expression for V has a horizontal asymptote of 0 and a vertical asymptote at $\rho = [1 - (g_s/g_r)^2]^{-1}$, i.e., ρ is only slightly greater than 1. With reference to the data in Figs. 2–6, the left axis is on the "flat" portion of the graph, the right axis is close to the asymptote and on the "steep" portion. Thus the plots are qualitatively similar to those predicted by the simplified model.

This work was supported by U.S. Public Health Service grants HL 32145 (RC) and AR39643 (EP), and a grant from the Muscular Dystrophy Association (RC). Portions of this work were carried out while EP was an American Heart Association Established Investigator. GC gratefully acknowledges the support of the Italian Telethon Project 474.

REFERENCES

Adelstein, R. S., and C. B. Klee. 1981. Purification and characterization of smooth muscle myosin light chain kinase. *J. Biol. Chem.* 256: 7501–7509.

Brenner, B. 1990. Muscle mechanics and biochemical kinetics. *In* Molecular Mechanisms in Muscular Contraction. J. M. Squire, editor. Macmillan Press, London. 77–149.

Brenner, B., and E. Eisenberg. 1986. Rate of force generation in muscle: correlation with actomyosin ATPase activity in solution. *Proc. Natl. Acad. Sci. USA.* 83:3542–3546.

Brenner, B., M. Schoenberg, J. M. Chalovich, L. E. Greene, and E. Eisenberg. 1982. Evidence for cross-bridge attachment in relaxed muscle at low ionic strength. *Proc. Natl. Acad. Sci. USA.* 79:7288–7291.

Brokaw, C. J. 1976. Computer simulation of movement generating cross-bridges. *Biophys. J.* 16:1013–1027.

Chalovich, J. M., L. E. Greene, and E. Eisenberg. 1983. Cross-linked myosin subfragment 1: a stable analogue of the subfragment-1·ATP complex. *Proc. Natl. Acad. Sci. USA.* 80:4909–4913.

Chase, P. B., D. A. Martyn, M. J. Kushmerick, and A. M. Gordon. 1993. Effects of inorganic phosphate analogs on stiffness and unloaded short-

ening of skinned muscle fibres from rabbit. *J. Physiol. (Lond.).* 460: 231–246.

Cooke, R. 1986. The mechanism of muscle contraction. *CRC. Crit. Rev. Biochem.* 21:53–118.

Daniel, J. L., and J. R. Sellers. 1992. Purification and characterization of platelet myosin. *Methods Enzymol.* 215:78–88.

Dantzig, J. A., and Y. E. Goldman. 1986. Supression of muscle contraction by vanadate. Mechanical and ligand binding studies on glycerol-extracted rabbit fibres. *J. Gen. Physiol.* 86:305–327.

Dillon, P. F., M. O. Aksoy, S. P. Driska, and R. A. Murphy. 1981. Myosin phosphorylation and the cross-bridge cycle in arterial smooth muscle. *Science.* 211:495–497.

Eisenberg, E., T. L. Hill, and Y. Chen. 1980. Cross-bridge model of muscle contraction. *Biophys. J.* 29:195–227.

Eisenberg, E., and W. W. Kielley. 1974. Troponin-tropomyosin complex. *J. Biol. Chem.* 249:4742–4748.

Ganguly, C., I. C. Baines, E. D. Korn, and J. R. Sellers. 1992. Regulation of the actin-activated ATPase and in vitro motility activities of monomeric and filamentous *Acanthamoeba* myosin II. *J. Biol. Chem.* 267: 20900–20904.

Goldman, Y. E. 1993. Kinetics of the actomyosin ATPase in muscle fibers. *Annu. Rev. Physiol.* 49:637–654.

Greene, L. E., and J. R. Sellers. 1987. Effect of phosphorylation on the binding of smooth muscle heavy meromyosin·ADP to actin. *J. Biol. Chem.* 262:4177–4181.

Guilford, W. H., M. J. Tyska, Y. Freyzon, and D. M. Warshaw. 1996. Smooth muscle myosin with an elongated neck region produces greater unitary displacement in vitro. *Biophys. J.* 70:A127.

Hai, C.-M., and R. A. Murphy. 1989. Ca^{2+}, cross-bridge phosphorylation, and contraction. *Annu. Rev. Physiol.* 51:285–298.

Harris, D. E., and D. M. Warshaw. 1993a. Smooth and skeletal muscle actin are mechanically indistinguishable in the in vitro motility assay. *Circ. Res.* 72:219–224.

Harris, E. E., and D. M. Warshaw. 1993b. Smooth and skeletal muscle myosin both exhibit low duty cycles at zero load in vitro. *J. Biol. Chem.* 268:14764–14768.

Harris, D. E., S. S. Work, R. K. Wright, N. R. Alpert, and D. M. Warshaw. 1994. Smooth, cardiac and skeletal muscle myosin force and motion generation assessed by cross-bridge mechanical interactions in vitro. *J. Muscle Res. Cell Motil.* 15:11–19.

Herzig, J. W., J. W. Peterson, J. C. Ruegg, and R. J. Solaro. 1981. Vanadate and phosphate ions reduce tension and increase cross-bridge kinetics in chemically-skinned heart muscle. *Biochim. Biophys. Acta.* 726:13–39.

Hoh, J. F. Y., P. A. McGrath, and P. T. Hale. 1993. Electrophoretic analysis of multiple forms of rat cardiac myosin: effect of hypophysectomy and thyroxine replacement. *J. Mol. Cell. Cardiol.* 10:1053–1076.

Homsher, E., F. Wang, and J. R. Sellers. 1992. Factors affecting movement of F-actin filaments propelled by skeletal muscle heavy meromyosin. *Am. J. Physiol. Cell Physiol.* 262:C714–C723.

Huxley, A. F. 1957. Muscle structure and theories of contraction. *Prog. Biophys. Biophys. Chem.* 7:255–318.

Klee, C. B. 1977. Conformational transition accompanying the binding of Ca^{2+} to the protein activator of 3′,5′-cyclic adenosine monophosphate phosphodiesterase. *Biochemistry.* 16:1017–1024.

Kron, S. J., and J. A. Spudich. 1986. Fluorescent actin filaments move on myosin fixed to a glass surface. *Proc. Natl. Acad. Sci. USA.* 83: 6272–6276.

Larsson, L., and R. L. Moss. 1993. Maximum velocity of shortening in relation to myosin isoform composition in single fibres from human skeletal muscles. *J. Physiol. (Lond.).* 472:595–614.

Luo, Y., R. Cooke, and E. Pate. 1993. Stress relaxation in cross-bridge systems containing a series elastic element. *Am. J. Physiol.* 265: C279–C288.

Margossian, S. S., and S. Lowey. 1982. Preparation of myosin and its subfragments from rabbit skeletal muscle. *Methods Enzymol.* 85:55–71.

Millar, N. C., and Homsher, E. 1992. Kinetics of force generation and phosphate release in skinned rabbit soleus muscle fibers. *Am. J. Physiol.* 262:C1239–C1245.

Okagaki, T., S. Higashi-Fujime, and K. Kohama. 1989. Ca^{2+} activates actin-filament sliding on scallop myosin but inhibits that on *Physarum* myosin. *J. Biochem. (Tokyo).* 106:955–957.

Pate, E., and R. Cooke. 1989. A model of cross-bridge action, the effects of ATP, ADP and P_i. *J. Muscle Res. Cell Motil.* 10:181–196.

Pate, E., and R. Cooke. 1991. Simulation of stochastic processes in motile crossbridge systems. *J. Muscle Res. Cell Motil.* 12:376–393.

Pate, E., H. White, and R. Cooke. 1993. Determination of the myosin step size from mechanical and kinetic data. *Proc. Natl. Acad. Sci. USA.* 90:2451–2455.

Perrie, W. T., and S. V. Perry. 1970. An electrophoretic study of the low-molecular-weight components of myosin. *Biochem. J.* 119:31–38.

Schoenberg, M. 1988. Characterization of the myosin adenosine triphosphate (M·ATP) cross-bridge in rabbit and frog skeletal muscle fibers. *Biophys. J.* 54:135–148.

Sellers, J. R. 1985. Mechanism of the phosphorylation-dependent regulation of smooth muscle heavy meromyosin. *J. Biol. Chem.* 260: 15815–15819.

Sellers, J. R., and Goodson, H. W. 1995. Motor proteins 2: myosin. *Protein Profile.* 2:1323–1423.

Sellers, J. R., and B. Kachar. 1990. Polarity and velocity of sliding filaments: control of direction by actin and of speed by myosin. *Science.* 249:406–408.

Sellers, J. R., J. A. Spudich, and M. P. Sheetz. 1985. Light chain phosphorylation regulates the movement of smooth muscle myosin on actin filaments. *J. Cell Biol.* 101:1897–1902.

Siemenkowski, R. F., M. O. Wiseman, and H. W. White. 1985. ADP dissociation from actomyosin subfragment 1 is sufficiently slow to limit the inloaded shortening velocity in vertebrate muscle. *Proc. Natl. Acad. Sci. USA.* 82:658–662.

Umemoto, S., A. R. Bengur, and J. R. Sellers. 1989. Effect of multiple phosphorylations of smooth muscle and cytoplasmic myosins on movement in an in vitro motility assay. *J. Biol. Chem.* 264:1431–1436.

Umemoto, S., and J. R. Sellers. 1990. Characterization of in vitro motility assays using smooth muscle and cytoplasmic myosins. *J. Biol. Chem.* 265:14864–14869.

Uyeda, T. Q. P., S. J. Kron, and J. A. Spudich. 1990. Myosin step size. Estimation from slow sliding movement of actin over low densities of heavy meromyosin. *J. Mol. Biol.* 214:699–710.

VanBuren, P., D. E. Harris, N. R. Alpert, and D. M. Warshaw. 1995. Cardiac V_1 and V_3 myosins differ in their hydrolytic and mechanical activities in vitro. *Circ. Res.* 77:439–444.

VanBuren, P., S. S. Work, and D. M. Warshaw. 1993. Enhanced force generation by smooth muscle myosin. *Proc. Natl. Acad. Sci. USA.* 91:202–205.

Wang, D., E. Pate, R. Cooke, and R. Yount. 1993a. Synthesis of nonnucleotide ATP analogues and characterization of their chemomechanical interaction with muscle fibers. *J. Muscle Res. Cell Motil.* 14:484–497.

Wang, F., B. M. Martin, and J. R. Sellers. 1993b. Regulation of actomyosin interactions in *Limulus* muscle proteins. *J. Biol. Chem.* 268:3776–3780.

Warshaw, D. M., J. M. Desrosiers, S. S. Work, and K. M. Trybus. 1990. Smooth muscle myosin cross-bridge interactions modulate actin filament sliding velocity in vitro. *J. Cell Biol.* 111:453–463.

Yamakawa, M., D. E. Harris, F. S. Fay, and D. M. Warshaw. 1990. Mechanical transients of single toad stomach smooth muscle cells. *J. Gen. Physiol.* 95:697–715.

Yamashita, H., S. Sugiura, T. Serizawa, T. Sugimoto, M. Iizuka, E. Katayama, and T. Shimmen. 1992. Sliding velocity of isolated rabbit cardiac myosin correlates with isozyme distribution. *Am. J. Physiol. Heart Circ. Physiol.* 263:H464–H472.